

SHORT COMMUNICATION

O-18. COMPATIBILITY OF FLUOROCHROME LABELING PROTOCOL WITH RAMAN SPECTROSCOPY TO STUDY BONE FORMATION.

C. Olejnik^{1,2}, G. Falgayrac¹, A. During¹, G. Penel^{1,2}

¹Université Lille Nord de France, EA4490, PMOI, Faculté de Chirurgie dentaire, Pl. de Verdun, Lille, France. ²Service d'Odontologie, CHRU de Lille, Pl. de Verdun, Lille, France.

Keys Words

Bone mineralization, Raman microscopy, Fluorescent dyes

Introduction

Raman microspectroscopy (RM) is increasingly recognized as an efficient method to bring new information on the composition and structure of mineralized tissues. Physicochemical parameters (mineralization, carbonation and cristallinity) measured from RM bands provide information in bone quality changes due to aging or pathologies (1, 2, 3). In vivo models have been extensively used to investigate bone remodeling and healing. Cranial bone defect models especially are reported to test cell implantation, growth factors or biomaterials (4, 5, 6, 7). The bone process healing can be followed by sequential fluorochrome labelings within animal model. Calcium-binding fluorochromes are incorporated at sites of active mineralization (8, 9). RM is non-destructive technique that allows analyses of different points of a single sample. Despite these advantages, the fixation and embedding procedures of a biological sample can interfere with RM signal (10). Furthermore, fluorescent background noise is one of the major drawback of the RM technique. The sample preparation procedures can generate these artifacts and preclude the RM signal detection. The compatibility of histological stains (e.g. hematoxylin, eosin) has been investigated (11) but no current study has been carried out on fluorescent dyes (e.g. calcein, demeclocycline) effects on Raman spectra. The aim of this study was thus to determinate the compatibility between fluorescence and RM in an in vivo model of cranial bone defect healing.

Materials and methods

Rat model: Surgical standardized bone calvaria defect on adult Sprague Dawley rats were performed (4). A 4-mm-diameter defect was performed with a trephine burr on sagittal suture. Calcein and demeclocycline (Sigma Chemical, St Louis, MO, USA) were injected intramuscularly at the 13th and 27th postoperative days respectively, at the dose of 30 mg/kg body weight. Rats were killed 28th day postoperative and calvaria were harvested.

Samples preparation: Samples were fixed 24h in 70% ethanol and embedded in Polymethylmethacrylate (PMMA). 100 μ m thick sections were cut and polished. An epifluorescence confocal microscope (LSM 710, Carl Zeiss Inc.) was used for the new bone formation localization. Photomultiplier filters of 494 nm wavelength for calcein and 535 nm wavelength for demeclocycline were used.

Raman analyses: A Labram confocal microspectrometer (Horiba Gr, Jobin Yvon, Lille, France) was used to acquire spectra. Raman spectra were obtained with a helium-neon laser ($\lambda=632.82$ nm) and an objective x100 (NA=0.80). The set of acquisitions was performed in a range of 800–1750 cm^{-1} . Raman spectra were acquired over area 8x8 μ m by steps of 2 μ m. For each point, the spectrum was the result of 3 accumulations with an integration time of 45s. Fluorescent (test, n=4) and no-fluorescent (control, n=4) areas were analysed in both neo-formed and native bone.

Results

Microscopic fluorescence images represent the regions of calcium precipitation during bone mineralization (Fig. 1). In bone defect, isolated spread mineralized sites can be loca-

lized, with distinct labelling corresponding to different mineralization periods. Whereas at distance, periosteal remodeling is observed as a linear apposition and discrimination between 2 labelling was not possible. Both sites (i.e. defect and distant) were analyzed by Raman spectroscopy. The signal-to-noise ratio was efficient and typical spectra were obtained in all localizations (Fig. 2). Fluorescent dyes don't interfere with bone spectrum: no shift band or overlaps with fluorescent peak were observed.

Discussion

Spectroscopic studies have evaluated bone formation with multiple fluorochromes whe-

re mineralization front was spatially distinct. The collected spectrum was performed from the area between the two labels (12, 13). In healing bone defect, bone reconstruction is a dynamic and 3-dimensionnal process where separation between labeled areas is hardly obtained. Fluorochromes available for bone formation labelling exhibit different affinity for the tissue and different peak emission wavelength. For example, alizarin considered as having greatest affinity to calcium (14), has a maximum emission at 624–645 nm (8) which might enhance the background noise with helium-neon laser ($\lambda=632.82$ nm) use in the present work. In addition, the complete emission wavelength has to be separate in the range of 20 nm by conventional imaging microscopy to allow the detection of 2 different labeling (9). All these points should be considered for coupling with RM investigation as the labeling should generate emission of fluorescence noise or additional bands. In this work, successful RM analyses have been carried out within the labeled areas.

Conclusion

The present work demonstrates the ability of Raman microspectrometry to be used for investigation of new bone formation labeled with tetracycline derivates. This method should be of a great help for mineralization process and bone maturation studies in different physiopathological situations and chemometric analyses should be performed in such purpose.

Acknowledgements

We would like to thank the Institut Français pour la Recherche en Odontologie (IFRO) for its financial support.

References

1. Gamsjaeger S et al. (2010) Bone, 47:392-399.
2. Yerramshetty JS et al. (2006) Bone, 39:1236-1242.
3. Morris MD et al. (2011) Clin Orthop Relat Res, 469:2160-2169.
4. Nagata M et al. (2009) Bone, 45:339-345.
5. Guskuma MH et al. (2010) J appl Oral Sci, 18:346-53.

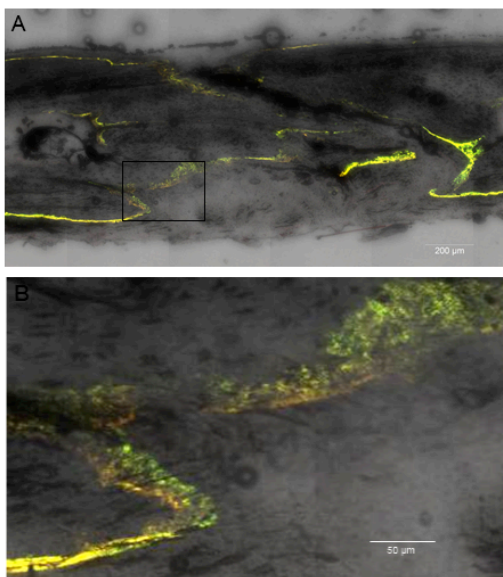


Fig. 1. Photomicrographs of calcein (green) and demeclocycline (red) labeled defect sites (A) total area, (B) detail area, where Raman acquisitions are performed.

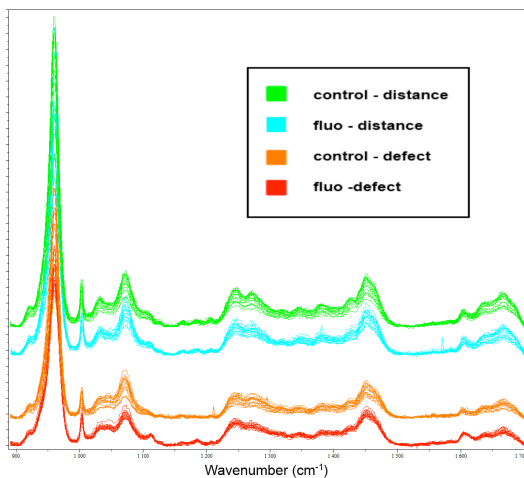


Fig. 2. Classical spectra obtained in each area.

6. Park JW et al. (2009) *Clin Oral Impl Res*, 20:372-378.
7. Pang EK et al. (2004) *J Periodontol*, 75:1364-1370
8. Pautke C et al. (2005) *Bone*, 37:441-445.
9. Pautke C et al. (2010) *J Anat*, 217:76-82.
10. Yeni YN et al. (2006) *Calcif Tissue Int*, 78:363-371.
11. Morris MD et al. (2004) *Calcif Tissue Int*, 74:86-94.